British Journal of Pharmacology

DOI:10.1111/bph.13342
www.brjpharmacol.org

RESEARCH PAPER

Characterization of 12 GnRH peptide agonists – a kinetic perspective

Indira Nederpelt[1], Victoria Georgi[2], Felix Schiele[2], Katrin Nowak-Reppel[2], Amaury E. Fernández-Montalván[2], Adriaan P. IJzerman[1] and Laura H. Heitman[1]

[1]*Division of Medicinal Chemistry, Leiden Academic Centre for Drug Research (LACDR), Leiden University, Leiden, The Netherlands, and* [2]*Global Drug Discovery, Lead Discovery Berlin, Bayer Healthcare Pharmaceuticals, Berlin, Germany*

Correspondence
Laura H. Heitman, Division of Medicinal Chemistry, Leiden University, Einsteinweg 55, 2333 CC Leiden, The Netherlands.
E-mail: l.h.heitman@lacdr.leidenuniv.nl

Received
23 December 2014
Revised
4 September 2015
Accepted
9 September 2015

BACKGROUND AND PURPOSE

Drug-target residence time is an important, yet often overlooked, parameter in drug discovery. Multiple studies have proposed an increased residence time to be beneficial for improved drug efficacy and/or longer duration of action. Currently, there are many drugs on the market targeting the gonadotropin-releasing hormone (GnRH) receptor for the treatment of hormone-dependent diseases. Surprisingly, the kinetic receptor-binding parameters of these analogues have not yet been reported. Therefore, this project focused on determining the receptor-binding kinetics of 12 GnRH peptide agonists, including many marketed drugs.

EXPERIMENTAL APPROACH

A novel radioligand-binding competition association assay was developed and optimized for the human GnRH receptor with the use of a radiolabelled peptide agonist, [^{125}I]-triptorelin. In addition to radioligand-binding studies, a homogeneous time-resolved FRET Tag-lite™ method was developed as an alternative assay for the same purpose.

KEY RESULTS

Two novel competition association assays were successfully developed and applied to determine the kinetic receptor-binding characteristics of 12 high-affinity GnRH peptide agonists. Results obtained from both methods were highly correlated. Interestingly, the binding kinetics of the peptide agonists were more divergent than their affinities with residence times ranging from 5.6 min (goserelin) to 125 min (deslorelin).

CONCLUSIONS AND IMPLICATIONS

Our research provides new insights by incorporating kinetic, next to equilibrium, binding parameters in current research and development that can potentially improve future drug discovery targeting the GnRH receptor.

Abbreviations

CHOhGnRH, CHO cells stably expressing the human GnRH receptor; GnRH, gonadotropin-releasing hormone; k_1, the association rate constant of the radioligand; k_2, the dissociation rate constant of the radioligand; k_3, the association rate constant of the unlabelled ligand; k_4, the dissociation rate constant of the unlabelled ligand; RT, residence time; TR-FRET, time-resolved FRET

Tables of Links

TARGETS
GnRH receptors

LIGANDS		
^{125}I-triptorelin	Goserelin	Nafarelin
Buserelin	Leuprorelin	Triptorelin
GnRH		

These Tables list key protein targets and ligands in this article which are hyperlinked to corresponding entries in http://www.guidetopharmacology.org, the common portal for data from the IUPHAR/BPS Guide to PHARMACOLOGY (Pawson *et al.*, 2014) and are permanently archived in the Concise Guide to PHARMACOLOGY 2013/14 (Alexander *et al.*, 2013).

Introduction

Drug-target residence time is emerging as an important parameter in the drug discovery process. Multiple studies provide evidence that the binding kinetics of drug-target interactions rather than the typical equilibrium binding parameters are important for *in vivo* efficacy (Swinney, 2004; Copeland *et al.*, 2006; Tummino and Copeland, 2008; Zhang and Monsma, 2009). Several marketed drugs in the field of GPCRs have retrospectively been shown to display slow receptor dissociation rates or, in other words, long receptor residence times (Guo *et al.*, 2014). For instance, the histamine H_1 receptor antagonist desloratidine was found to have a long residence time, which could explain its high potency and 24 h duration of action observed in clinical studies (Anthes *et al.*, 2002). Another example is the insurmountable antagonist for the angiotensin AT_1 receptor, telmisartan. The authors deemed the insurmountability and therefore improved efficacy of telmisartan to be partly due to its very slow dissociation from AT_1 receptors (Maillard *et al.*, 2002).

The hypothalamic neuropeptide gonadotropin-releasing hormone (GnRH) is a central mediator of reproductive functions. This decapeptide binds to a class A GPCR, namely, the GnRH receptor located mainly on pituitary gonadotrophs. Along with the pituitary, GnRH receptors are expressed in reproductive tissues, both normal and malignant, such as those of the prostate and mammary gland (Kakar *et al.*, 1994; von Alten *et al.*, 2006; Angelucci *et al.*, 2009; Aguilar-Rojas *et al.*, 2012). Upon receptor activation, the gonadotropins luteinizing hormone (LH) and follicle-stimulating hormone (FSH) are synthesized and secreted from gonadotrophic cells. LH and FSH consecutively induce follicle stimulation and ovulation in women and promote steroidogenesis in both men and women (Stojilkovic *et al.*, 1994).

The pulsatile release of GnRH from the hypothalamus is essential for the maintenance of ovarian function. Sustained exposure of GnRH receptors to GnRH or GnRH analogues leads to activation, commonly named 'flare', followed by desensitization of GnRH receptor-mediated gonadotropin secretion. Accordingly, blockade by antagonists and desensitization of GnRH receptor-mediated gonadotropin secretion both ultimately reduce circulating levels of gonadotropins and gonadal steroids (Belchetz *et al.*, 1978; Lahlou *et al.*, 1987). This so-called chemical castration underlies the therapeutic use of GnRH analogues to treat sex hormone-dependent diseases (Depalo *et al.*, 2012; Labrie, 2014; Leone Roberti Maggiore *et al.*, 2014).

Consequently, considerable efforts have been put towards the development of agonists and antagonists targeting the GnRH receptor (Karten and Rivier, 1986; Sealfon *et al.*, 1997; Millar *et al.*, 2004; Heitman and IJzerman, 2008; Millar and Newton, 2013). Only a few studies have examined the receptor-binding kinetics of GnRH ligands. A paper of Heise *et al.* (2007) described a scintillation proximity assay to qualitatively distinguish between fast and slowly dissociating antagonists for the GnRH receptor. The authors demonstrated that slow dissociation rates were responsible for large discrepancies between a ligand's K_i value determined at 30 min versus 10 h, and they suggested using the K_i ratio as a screening method to select slowly dissociating compounds. Two other studies focused on a quantitative determination of receptor-binding kinetics of small molecule GnRH antagonists. Here, a direct correlation between the insurmountability and slow dissociation rates of these antagonists was shown (Sullivan *et al.*, 2006; Kohout *et al.*, 2007).

Currently, multiple peptide GnRH analogues have been approved for the treatment of advanced prostatic cancer, endometriosis, *in vitro* fertilization and more (Depalo *et al.*, 2012; Romero *et al.*, 2012; Aydiner *et al.*, 2013; Goericke-Pesch *et al.*, 2013; Lewis *et al.*, 2013; Labrie, 2014; Leone Roberti Maggiore *et al.*, 2014). Remarkably, the receptor-binding kinetics of peptide GnRH receptor ligands have never been reported. Therefore, we developed a novel radioligand-binding competition association assay that allowed us to determine the kinetic binding parameters and focused on 12 GnRH peptide agonists, including many marketed drugs (Table 1). In addition, we compared these kinetic parameters with those from a newly developed homogeneous time-resolved fluorescent assay. Both assays may improve future drug discovery targeting the GnRH receptors by incorporating kinetic receptor-binding parameters into current research and development trajectories.

Methods

Cell culture

For radioligand-binding assays, CHOhGnRH cells were grown in Ham's F12/DMEM (1:1) medium supplemented with 10% normal bovine serum, 2 mM glutamine, penicillin (100 IU·mL^{-1}), streptomycin (100 µg·mL^{-1}) and G418 (200 µg·mL^{-1}) at 37°C in 5% CO_2.

Table 1

Amino acid sequences of the 12 GnRH peptide agonists examined

	1	2	3	4	5	6	7	8	9	10
GnRH	pGlu*	His	Trp	Ser	Tyr	**Gly**	Leu	Arg	Pro	**Gly–NH_2**
Triptorelin	pGlu*	His	Trp	Ser	Tyr	**D-Trp**	Leu	Arg	Pro	**Gly–NH_2**
[D-Ala^6]-GnRH	pGlu*	His	Trp	Ser	Tyr	**D-Ala**	Leu	Arg	Pro	**Gly–NH_2**
[D-Lys^6]-GnRH	pGlu*	His	Trp	Ser	Tyr	**D-Lys**	Leu	Arg	Pro	**Gly-NH_2**
Fertirelin	pGlu*	His	Trp	Ser	Tyr	**Gly**	Leu	Arg	Pro	**NHEt***
Alarelin	pGlu*	His	Trp	Ser	Tyr	**D-Ala**	Leu	Arg	Pro	**NHEt***
Deslorelin	pGlu*	His	Trp	Ser	Tyr	**D-Trp**	Leu	Arg	Pro	**NHEt***
Leuprorelin	pGlu*	His	Trp	Ser	Tyr	**D-Leu**	Leu	Arg	Pro	**NHEt***
Nafarelin	pGlu*	His	Trp	Ser	Tyr	**D2Nal**	Leu	Arg	Pro	**Gly–NH_2**
Buserelin	pGlu*	His	Trp	Ser	Tyr	**Ser-tBu***	Leu	Arg	Pro	**NHEt***
Goserelin	pGlu*	His	Trp	Ser	Tyr	**Ser-tBu***	Leu	Arg	Pro	**azaGly–NH_2***
Histerelin	pGlu*	His	Trp	Ser	Tyr	**His(Bzl)***	Leu	Arg	Pro	**NHEt***

The differences between the peptides are expressed in bold

*pGlu, pyroglutamic acid; D2Nal, (2-naphthyl)-D-alanine; Ser-tBu, serine-tert-butyl; His(Bzl), N-benzyl-L-histidine; azaGly–NH_2, aza-glycine amine; NHEt, ethylamide

For time-resolved FRET (TR-FRET) experiments, 1 mL ($7 * 10^6$ cells·mL^{-1}) of Tag-lite GnRH cells were thawed, washed with 15 mL ice-cold Tag-lite buffer (TLB), resuspended in 5 mL TLB and immediately used.

Membrane preparation

CHOhGnRH cells were scraped from the plates in 5 mL PBS, collected and centrifuged at 700× *g* for 5 min. Derived pellets were pooled and resuspended in 50 mM Tris HCl buffer pH 7.4 at 25°C supplemented with 2 mM $MgCl_2$ and subsequently homogenized with an UltraThurrax (Heidolph Instruments, Schwabach, Germany). The cytosolic fraction and membranes were separated by centrifugation at 100 000× *g* in an Optima LE-80 K ultracentrifuge (Beckman Coulter, Fullterton, CA, USA) for 20 min at 4°C. The pellet was resuspended, and centrifugation was repeated. The obtained pellet was resuspended; membranes were aliquoted and stored at −80°C. Membrane protein concentrations were determined using the bicinchoninic acid method with BSA as a standard (Smith *et al.*, 1985).

Radioligand equilibrium assays

Displacement experiments were performed as previously reported (Heitman *et al.*, 2008). In short, membrane aliquots containing 15–20 μg protein were incubated in a total volume of 100 μL assay buffer (25 mM Tris HCl, pH 7.4 at 25°C, supplemented with 2 mM $MgCl_2$, 0.1% (w v^{-1}) BSA) at 25°C for 2 h. Ten concentrations of competing ligand were used in the presence of 30.000 c.p.m. (~0.1 nM) [^{125}I]-triptorelin. At this concentration, total radioligand binding did not exceed 10% of that added to prevent ligand depletion. Non-specific binding was determined in the presence of an excess amount of GnRH (1 μM). The reaction was terminated by the addition of 1 mL ice-cold wash buffer (25 mM Tris HCl, pH 7.4 at 25°C, supplemented with 2 mM $MgCl_2$ and 0.05% (w v^{-1}) BSA). Separation of bound from free radioligand was performed by rapid filtration through Whatman GF/B filters saturated with 0.25% polyethylene imine using a Brandel harvester. Filters were subsequently washed three times with 2 mL ice-cold wash buffer. Filter bound radioactivity was determined using a γ-counter (Wizard 1470, PerkinElmer).

Radioligand kinetic association and dissociation assays

Association experiments were carried out by incubating membrane aliquots containing 15–20 μg protein in a total volume of 100 μL assay buffer at 25°C with 30.000 c.p.m. (~0.1 nM) [^{125}I]-triptorelin. The amount of radioligand bound to the receptor was determined at different time intervals for a total incubation time of 120 min.

Dissociation experiments were performed by pre-incubating membrane aliquots containing 15–20 μg protein in a total volume of 100 μL assay buffer at 25°C for 45 min with 30.000 c.p.m. (~0.1 nM) [^{125}I]-triptorelin. After pre-incubation, dissociation was initiated by addition of an excess amount of GnRH (1 μM) in a total volume of 2.5 μL. The amount of radioligand still bound to the receptor was measured at various time intervals for a total incubation time of 120 min. The reaction was stopped, and samples were harvested as described under Radioligand Equilibrium Assays.

Radioligand kinetic competition association assays

The binding kinetics of unlabelled ligands were quantified using the competition association assay based on the method by Motulsky and Mahan (1984). During optimization, three different concentrations of unlabelled triptorelin were tested; 0.3-fold, 1-fold and 3-fold its K_i value. The kinetic parameters

of all other unlabelled ligands were determined at a concentration of onefold their K_i, unless stated otherwise. The competition association assay was initiated by adding membrane aliquots containing 15–20 μg protein in a total volume of 100 μL assay buffer at 25°C with 50.000 c.p.m. (~0.15 nM) [^{125}I]-triptorelin in the absence or presence of competing ligand. Of note, total radioligand binding did not exceed 10% of that added at this concentration to prevent ligand depletion. The amount of radioligand bound to the receptor was determined at different time intervals for a total incubation time of 120 min. The reaction was stopped, and samples were harvested as described under Radioligand Equilibrium Assays.

TR-FRET probe equilibrium assays

Unless otherwise specified, TR-FRET measurements were carried out using the conditions described in Schiele *et al.* (2014). To determine the equilibrium affinity of the fluorescent probe, 5 μL Tag-lite GnRH cells (1400 cells·μL^{-1}) were incubated for 1 h, to ensure signal stability, with increasing probe concentrations (ranging from 0 to 100 nM: Supporting Information Fig. S1) in a final volume of 10 μL. In parallel, a non-specific binding control was carried out in the presence of an excess amount of buserelin (100 μM). Binding signals were measured in a PHERAstar FS plate reader BMG Labtech (Offenburg, Germany) by exciting the Tb donor with five laser flashes at a wavelength of 337 nm and recording acceptor and donor emission fluorescence channels (A and B channels), at wavelengths of 520 and 490 nm respectively.

TR-FRET equilibrium probe competition assays

'Ready-to-use' assay plates containing serial dilutions of the test agonists were prepared as described in Schiele *et al.* (2014). Subsequently, 5 μL Tag-lite GnRH cells (1400 cells·μL^{-1}) and 50 nM probe were added to the competitors and incubated at room temperature for 1 h, to ensure signal stability, in a final volume of 10 μL. Non-specific binding ('low signal') controls contained an excess amount of buserelin (100 μM), whereas in 'high signal' controls, the test compounds were replaced by DMSO. Binding signals were recorded as described under TR-FRET Probe Equilibrium Assays.

TR-FRET kinetic probe association and dissociation assays

Measurements were carried out in quadruplicate and in a final volume of 15 μL per well. First, a 5-point, twofold serial dilution of fluorescent probe (Supporting Information Fig. 2) was pre-dispensed on black 384-well low volume plates (Greiner Bio-one (Frickenhausen, Germany)), and the PHERAstar FS injection system's syringes (previously washed with NaOH/H_2O) were primed either with 1500 μL solution of Tag-lite GnRH cells (1000 cells·μL^{-1}) or with 200 μM buserelin. Then, 4 μL of cells were quickly added to the probe with the first syringe, and the association traces were recorded as described under TR-FRET Probe Equilibrium Assays, with kinetic intervals of 26 s. After 30 min, fluorescent probe dissociation was initiated by addition of 5 μL of an excess of unlabelled buserelin (final concentration 67 μM) with the second syringe, and the traces were recorded with kinetic intervals of 300 s in the same fashion. Alternatively, a 1-point measurement was performed with 5 μL of probe (final concentration 25 nM) and 5 μL of Tag-lite GnRH cells (1400 cells·μL^{-1}), and association was recorded with kinetic intervals of 120 s. After 24 min, dissociation was initiated and recorded with the same kinetic interval.

TR-FRET kinetic probe titration assays

First, 5 μL of increasing concentrations of fluorescent probe were dispensed into 384-well plates; the injection system of the PHERAstar FS plate reader was primed with Tag-lite GnRH cells as described under TR-FRET Probe Equilibrium Assays. Then, 5 μL of cell solution was added with the syringe, and the TR-FRET signals corresponding to probe association were recorded as described under TR-FRET Probe Equilibrium Assays.

TR-FRET kinetic probe competition assays

The basic principle of this assay is explained in Schiele *et al.* (2014). Before each experiment, 6 μL of fluorescent probe (final concentration 15 nM) was dispensed to the 'assay-ready' plates containing 100 nL of compound dilutions using a Multidrop Combi Thermo Fischer Scientific (Dreieich, Germany), and the injection system of the PHERAstar FS plate reader was washed with NaOH/H_20 and primed with Tag-lite GnRH cells. Finally, the assay plates were introduced into the instrument, 4 μL of cells (1000 cells·μL^{-1}) were rapidly dispensed with the syringe to each well and the TR-FRET signals corresponding to the competitive binding of probe and test compounds were recorded as described under TR-FRET Probe Equilibrium Assays with kinetic intervals of 78 s.

Data analysis

All experimental data were analysed using the nonlinear regression curve-fitting programme GraphPad Prism v. 5.00 (GraphPad Software Inc., San Diego, CA, USA). Further details on the handling of TR-FRET data are available in Schiele *et al.* (2014).

For radioligand-binding assays, the previously reported K_D value of 0.35 nM for [^{125}I]-triptorelin (Heitman *et al.*, 2008) was used to convert IC_{50} values obtained from competition curve analysis into K_i values with the help of the Cheng–Prusoff equation (Cheng and Prusoff, 1973):

$$K_i = IC_{50}/(1 + [\text{radioligand}]/K_D)$$

Likewise, a K_D value of 0.8 nM obtained for the 'red'-labelled buserelin by fitting the data from the TR-FRET probe equilibrium binding assay (Supporting Information Fig. S1) to the model 'One site – Specific binding' was used to convert IC_{50} values from TR-FRET experiments to K_i values.

The observed association rates (k_{obs}) derived from both assays were obtained by fitting association data using one-phase exponential association. The dissociation rates were obtained by fitting dissociation data to a one-phase exponential decay model. The k_{obs} values were converted into association rate (k_{on}) values using the following equation:

$$k_{on} = (k_{obs} - k_{off})/[\text{radioligand}]$$

The association and dissociation rates were used to calculate the kinetic K_D using the following equation:

$$K_D = k_{off}/k_{on}$$

To further validate probe affinity and kinetic rate constants, association data from kinetic probe titration experiments were fitted to the 'Association kinetics – two or more concentrations of hot' model (Supporting Information Fig. S2). The k_{on} obtained from these experiments and K_D from equilibrium binding were used to calculate k_{off} as described previously.

Association and dissociation rates for unlabelled ligands were calculated by fitting the data of the competition association assay using kinetics of competitive binding (Motulsky and Mahan, 1984):

$$K_A = k_1[L]\cdot 10^{-9} + k_2$$
$$K_B = k_3[I]\cdot 10^{-9} + k_4$$
$$S = \sqrt{(K_A - K_B)^2 + 4\cdot k_1\cdot k_3\cdot L\cdot I\cdot 10^{-18}}$$
$$K_F = 0.5(K_A + K_B + S)$$
$$K_S = 0.5(K_A + K_B - S)$$
$$Q = \frac{B_{max}\cdot k_1\cdot L\cdot 10^{-9}}{K_F - K_S}$$
$$Y = Q\cdot\left(\frac{k_4\cdot(K_F - K_S)}{K_F\cdot K_S} + \frac{k_4 - K_F}{K_F}e^{(-K_F\cdot X)} - \frac{k_4 - K_S}{K_S}e^{(-K_S\cdot X)}\right)$$

where k_1 is the k_{on} of the radioligand ($M^{-1}\cdot min^{-1}$), k_2 is the k_{off} of the radioligand (min^{-1}), L is the radioligand concentration (nM), I is the concentration of the unlabelled competitor (nM), X is the time (min) and Y is the specific binding of the radioligand (DPM). During a competition association, these parameters are set, obtaining k_1 from the control curve without competitor and k_2 from previously performed dissociation assays described under Radioligand Association and Dissociation Assays. With that, the k_3, k_4 and B_{max} can be calculated, where k_3 represents the k_{on} ($M^{-1}\cdot min^{-1}$) of the unlabelled ligand, k_4 stands for the k_{off} of the unlabelled ligand and B_{max} equals the total binding (DPM). All competition association data were globally fitted.

In case of kinetic probe competition assays (kPCA), the kinetics of the competitive binding model was enhanced with a mathematical term describing a mono-exponential decay that accounts for signal drift (Schiele *et al.*, 2014). As stated for the radioligand-binding assays, the kinetic rate constants of the fluorescent probe (k_1 and k_2) were determined in separate experiments and set constant in kPCA data analysis.

The RT was calculated as in the following equation:

$$RT = 1/k_{off}$$

All values obtained from radioligand-binding assays are means of at least three independent experiments performed in duplicate, unless stated otherwise. Values obtained from TR-FRET assays are means of two independent experiments performed in quadruplicate, unless stated otherwise.

Reagents and peptides

Deslorelin and fertirelin (Table 1) were obtained from Genway Biotech Inc. (San Diego, CA, USA) and American Peptide Company (Sunnyvale, CA, USA) respectively. All other peptide analogues (Table 1) and BSA were purchased from Sigma-Aldrich Chemie B.V. (Zwijndrecht, The Netherlands). Bicinchoninic acid protein assay reagent was obtained from Pierce Chemical Company (Rockford, IL, USA). [^{125}I]-triptorelin (specific activity 2200 Ci·mmol^{-1}) was purchased from PerkinElmer (Groningen, The Netherlands). CHO cells stably expressing the human GnRH receptor (from now on CHOhGnRH cells) were kindly provided by MSD (Oss, The Netherlands). Tag-lite™ HEK293 cells containing a stably

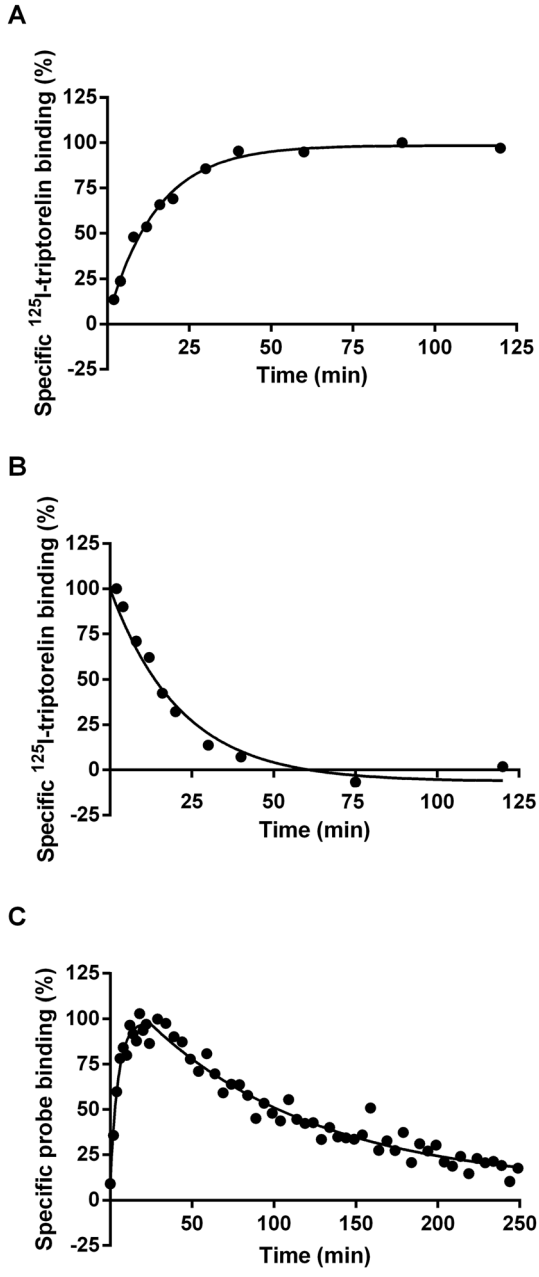

Figure 1

Association and dissociation kinetics of [^{125}I]-triptorelin (A,B) or fluorescent probe (C) at the hGnRH receptor. Representative graphs from one experiment performed in duplicate (see Tables 2 and 3 for kinetic parameters).

overexpressed human GnRH receptor labelled with Tb (from now on Tag-lite GnRH cells) were obtained as frozen stocks from Cisbio (Codolet, France). A buserelin-derived tracer, labelled at the sixth position with a red emitting fluorophore, and (TLB) were also purchased from Cisbio. All other chemicals and cell culture materials were obtained from standard commercial sources.

Results

Determination of the association and dissociation rate constants of [^{125}I]-triptorelin

The binding properties of [^{125}I]-triptorelin to CHOhGnRH membranes were quantified with traditional kinetic radioligand-binding assays. Association and dissociation experiments provided k_{on} and k_{off} values of 0.4 ± 0.1 $nM^{-1}{\cdot}min^{-1}$ and 0.05 ± 0.0004 min^{-1} respectively (Figure 1A and Table 2). From these data, the equilibrium dissociation constant (kinetic K_D) was calculated, which had a value of 0.2 nM.

Determination of the association and dissociation rate constants of the fluorescently labelled buserelin derivative probe

A fluorescently labelled buserelin derivative was used as a probe in all TR-FRET assays. The kinetic parameters of the fluorescent tracer were determined by performing association and dissociation experiments. Experiments yielded a k_{on} and k_{off} of 0.008 ± 0.001 $nM^{-1}{\cdot}min^{-1}$ and 0.01 ± 0.001 min^{-1} respectively (Figure 1B, Table 3 and Supporting Information Fig. 2). The kinetic K_D value calculated from these experiments was 1.2 nM.

Determination of the binding affinity of hGnRH receptor agonists with [^{125}I]-triptorelin

Equilibrium radioligand-binding assays were performed to assess the ability of 12 GnRH analogues to displace [^{125}I]-triptorelin from CHOhGnRH cell membranes. All ligands were able to fully displace [^{125}I]-triptorelin in a concentration-dependent manner (Figure 2A and Table 4). All peptides had a Hill coefficient close to unity in the [^{125}I]-triptorelin displacement assay (data not shown), which indicated a competitive mode of inhibition with regard to the radioligand. Of all tested ligands, nafarelin had the highest affinity for the hGnRH receptor with a K_i value of 0.06 nM, and GnRH had the lowest affinity of 13 nM. All other ligands had affinities in the low to sub-nanomolar range.

Determination of the binding affinity of hGnRH receptor agonists with TR-FRET

The binding affinity of 12 agonists was also determined using a fluorescently labelled buserelin derivative as a tracer and Tag-lite GnRH cells in a TR-FRET assay. In accordance with

Table 2

Comparison of the affinity, dissociation constants and kinetic parameters of reference agonist triptorelin obtained with different radioligand-binding assays

Assay	pK_D[b] and (K_D (nM))	pK_i and (K_i (nM))	k_{on} ($nM^{-1}{\cdot}min^{-1}$)	k_{off} (min^{-1})
Displacement	NA	9.6 ± 0.09 (0.27)	NA	NA
Association and dissociation	9.9 ± 0.11 (0.13)	NA	0.40 ± 0.12	0.050 ± 0.0004
Competition association[a]	9.7 ± 0.12 (0.22)	NA	0.12 ± 0.014	0.026 ± 0.008

Values are means ± SEM of three separate experiments performed in duplicate
NA, not applicable
[a]The binding kinetics of unlabelled triptorelin were determined by addition of 0.3-fold, 1-fold and 3-fold its K_i value
[b]$K_D = k_{off}/k_{on}$

Table 3

Comparison of the affinity, dissociation constants and kinetic parameters of the fluorescent buserelin probe obtained with different TR-FRET assays

Assay	pK_D and (K_D (nM))	pK_i and (K_i (nM))	k_{on} ($nM^{-1}{\cdot}min^{-1}$)	k_{off} (min^{-1})[b]
Equilibrium association	9.1 ± 0.8 (0.8)	NA	NA	NA
Association and dissociation[a]	8.9 ± 0.9 (1.2)	NA	0.008 ± 0.001	0.010 ± 0.001
Multiple association and dissociation	8.7 ± 0.06 (2.1)	NA	0.008 ± 0.001	0.016 ± 0.002

Values are means ± SEM of three separate experiments
NA, not applicable
[a]The dissociation kinetics of fluorescently labelled buserelin derivative were determined by addition of 10 μM buserelin
[b]$k_{off} = K_D$(equilibrium)$/k_{on}$

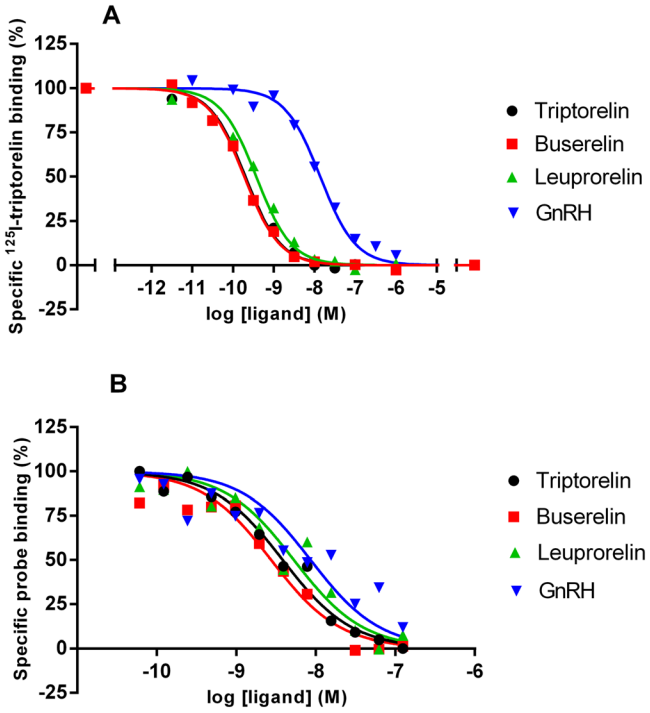

Figure 2

Displacement of [^{125}I]-triptorelin (A) or fluorescent probe (B) from the hGnRH receptor by the 12 peptide agonists. Representative graphs from one experiment performed in duplicate (see Table 4 for affinity values).

the radioligand-binding results, all agonists were able to fully displace the fluorescent tracer from the hGnRH receptor in a concentration-dependent manner (Figure 2B and Table 4). The data were in fair agreement with the affinities determined in the radioligand displacement assay despite the inherent differences between the two assays (r^2 = 0.5 and $P < 0.05$) (Figure 4C).

Validation and optimization of the competition association assay with [^{125}I]-triptorelin

With the k_{on} and k_{off} values of [^{125}I]-triptorelin obtained from traditional association and dissociation experiments, the k_{on} (k_3) and k_{off} (k_4) values of unlabelled triptorelin could be determined by fitting the kinetic parameters into the model of 'kinetics of competitive binding' as described under Methods. Three different concentrations of unlabelled triptorelin were tested and presented a shared k_{on} (k_3) and k_{off} (k_4) value of 0.1 ± 0.01 $nM^{-1}{\cdot}min^{-1}$ and 0.03 ± 0.008 min^{-1} respectively (Figure 3A). These values were in good agreement with the association and dissociation rates obtained with traditional kinetic experiments (Table 2). Additionally, a comparison of the affinity (0.3 nM) and dissociation constants (0.1 and 0.2 nM), acquired from equilibrium and kinetic experiments, respectively, further confirmed the competition association assay as a valid tool to determine the binding kinetics of unlabelled ligands at the hGnRH receptor (Table 2).

To improve the throughput of this assay, one concentration of competitor was selected that yielded an assay window discernable from both the baseline and control curve (i.e. specific binding approximately 40–60%). In this case, a concentration of competitor equal to onefold its K_i value presented the best assay window. Analysis of this single concentration

Table 4

Binding parameters of GnRH peptide agonists derived from radioligand binding and TR-FRET experiments

	Radioligand binding		TR-FRET	
Agonist	**pK_i and (K_i (nM))**	**pK_D and (K_D (nM))**	**pK_i and (K_i (nM))**	**pK_D and (K_D (nM))**
GnRH	7.9 ± 0.05 (13)	8.5 ± 0.08 (2.9)	8.4 ± 0.6 (4.0)	7.7 ± 0.03 (22)
Triptorelin	9.6 ± 0.09 (0.3)	9.7 ± 0.1 (0.2)	9.5 ± 0.2 (0.4)	9.5 ± 0.03 (0.4)
[D-Ala^6]-GnRH	9.0 ± 0.05 (0.8)	9.1 ± 0.09 (0.8)	8.6 ± 0.4 (2.3)	8.9 ± 0.02 (1.3)
[D-Lys^6]-GnRH	8.3 ± 0.1 (5.2)	8.4 ± 0.2 (3.7)$^{\#}$	7.8 ± 0.3 (16)	7.8 ± 0.01 (15)
Fertirelin	9.2 ± 0.05 (0.7)	9.1 ± 0.08 (0.8)$^{\#}$	9.0 ± 0.3 (1.0)	9.0 ± 0.02 (0.9)
Alarelin	9.4 ± 0.1 (0.5)	9.8 ± 0.1 (0.2)	9.0 ± 0.3 (0.9)	9.4 ± 0.03 (0.4)
Deslorelin	10 ± 0.1 (0.1)	9.9 ± 0.1 (0.1)$^{\#}$	8.6 ± 0.6 (0.8)	9.4 ± 0.04 (0.4)
Leuprorelin	9.5 ± 0.09 (0.3)	9.8 ± 0.1 (0.2)	9.7 ± 0.3 (0.2)	8.9 ± 0.03 (1.2)
Nafarelin	10 ± 0.06 (0.06)	10.6 ± 0.1 (0.03)	9.8 ± 0.3 (0.2)	9.7 ± 0.06 (0.2)
Buserelin	9.9 ± 0.05 (0.1)	10.4 ± 0.2 (0.04)	9.4 ± 0.2 (0.4)	9.5 ± 0.04 (0.3)
Goserelin	8.8 ± 0.06 (1.6)	9.0 ± 0.08 (1.1)	9.1 ± 0.3 (0.9)	8.6 ± 0.02 (2.7)
Histerelin	9.8 ± 0.2 (0.2)	10 ± 0.08 (0.04)	8.7 ± 0.5 (1.9)	9.0 ± 0.04 (1.0)

Values are means ± SEM of at least three separate experiments performed in duplicate
$^{\#}$Values are means ± SEM of two separate experiments performed in duplicate
$K_D = k_{off}/k_{on}$

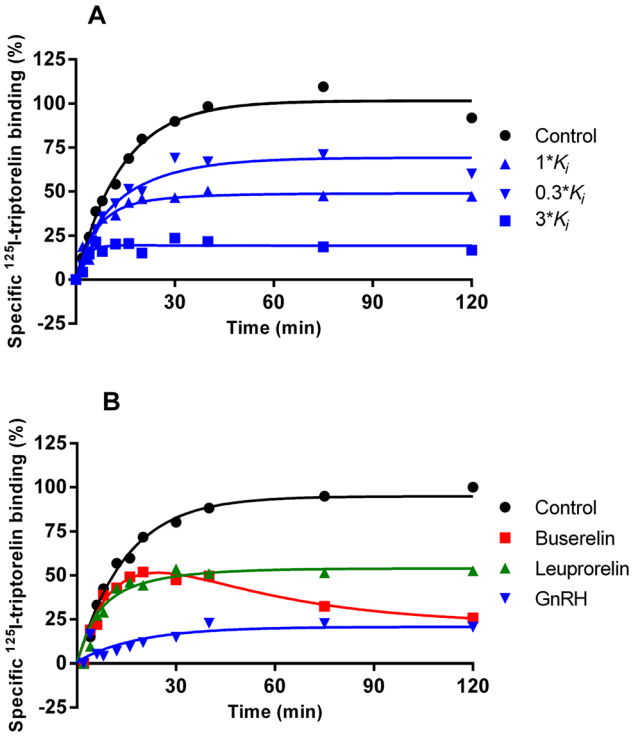

Figure 3

Competition association experiment with [^{125}I]-triptorelin in the absence or presence of 0.3, 1 or 3 * K_i value of unlabelled triptorelin (A) or 1 * K_i value of buserelin, leuprorelin or GnRH (B). Representative graphs from one experiment performed in duplicate (See Table 2 for kinetic parameters).

showed similar kinetic rates for triptorelin in comparison with the three-concentration method, which were statistically indifferent (data not shown; $P > 0.05$). Thus, this one-concentration method was used for subsequent determination of the binding kinetics of other unlabelled hGnRH receptor peptide agonists.

Determination of the receptor-binding kinetics of unlabelled hGnRH receptor agonists with [^{125}I]-triptorelin

By use of the one-concentration competition association assay, the binding kinetics of 11 other unlabelled hGnRH receptor agonists were quantified (Figure 3B and Table 5). Juxtaposing affinities (K_i values) and dissociation constants (K_D values) acquired from equilibrium and kinetic experiments resulted in a high correlation ($r^2 = 0.9$, $P < 0.0001$). Firstly, this further confirmed that the competition association assay was a valid tool to determine the binding kinetics of unlabelled ligands for the hGnRH receptor (Figure 4A) and, secondly, proved that equilibrium was reached for all agonists in the displacement experiments. The dissociation rates ranged from 0.2 ± 0.03 min^{-1} for goserelin to 0.01 ± 0.003 min^{-1} for buserelin, a variance of roughly 20-fold. Interestingly, three distinctive association patterns were obtained from the competition association assays (Figure 3B). Firstly, an 'overshoot' in [^{125}I]-triptorelin association was observed for slowly dissociating compounds, such as buserelin. Secondly, we noticed a shallow increase in [^{125}I]-triptorelin association for rapidly dissociating compounds, such as GnRH, and lastly, no difference was observed in the shape of the [^{125}I]-triptorelin association curve for equally fast-dissociating compounds, such as leuprorelin. The observed differences in dissociation kinetics were all in comparison with those of the radioligand [^{125}I]-triptorelin (Figure 3B). Association rates ranged from 0.8 ± 0.2 $nM^{-1}{\cdot}min^{-1}$ for nafarelin to 0.02 ± 0.004 $nM^{-1}{\cdot}min^{-1}$ for fertirelin, a span of approximately 35-fold.

Determination of the receptor-binding kinetics of unlabelled hGnRH receptor agonists with a fluorescently labelled buserelin derivative

The kinetic parameters of the 12 GnRH agonists were also determined with TR-FRET experiments (Figure 5, Table 5 and Supporting Information Fig. 3). Association rates ranged from 0.1 ± 0.02 $nM^{-1}{\cdot}min^{-1}$ for triptorelin to 0.02 ± 0.002 $nM^{-1}{\cdot}min^{-1}$ for histerelin. Buserelin was again one of the slowest dissociating agonists with a dissociation rate of 0.02 ± 0.003 min^{-1}, while GnRH had the fastest dissociation rate of 0.4 ± 0.03 min^{-1}. The dissociation constants (K_D) calculated from k_{on} and k_{off} values were consistent with the affinities determined in homogeneous time-resolved fluorescent displacement assays (Figure 4B) as well as with the K_D values obtained from the radioligand-binding studies (Figure 4D). Dissociation rate constants (k_{off}) were in good agreement with the data obtained from radioligand-binding experiments ($r^2 = 0.7$, $P < 0.0005$) (Figure 6A), while the association rates (k_{on}) presented no correlation ($r^2 = 0.03$, $P = 0.6$) (Figure 6B).

Discussion and conclusions

Over the years, several studies have indicated that long duration of action is an important feature contributing to improved efficacy of drugs designed to treat chronic illness. Moreover, increased target residence time offers the potential for a once-daily dosage form that increases patient compliance, which is crucial for the management of diseases (Smith *et al.*, 1996; Tashkin, 2005; Copeland *et al.*, 2006; Dowling and Charlton, 2006; Vauquelin and Van Liefde, 2006; Swinney, 2009; Zhang and Monsma, 2009; Guo *et al.*, 2014).

The GnRH receptor is the target of multiple marketed peptide agonists, classified as functional antagonists, used to treat hormone-dependent diseases. Available patient information for the most commonly prescribed GnRH analogues suggests that the pharmacokinetic/pharmacodynamics profiles are very similar. Hence, knowledge of the *in vitro* binding kinetics could give extra insights into these well-known drugs. However, the potential impact of variable-binding kinetics of these GnRH peptide derivatives on clinical efficacy has not been investigated. Aside from agonists, a few studies have detailed the effect of slow dissociation kinetics of antagonists for the GnRH receptor to decrease the maximal response of an agonist (insurmountability) *in vitro* and to improve and prolong efficacy *in vivo*. A study of Kohout and coworkers (2007) addressed the insurmountability of a small molecule GnRH antagonist, TAK-013. The authors examined

Table 5

Kinetic receptor-binding parameters of GnRH peptide agonists derived from radioligand-binding competition association assays and kPCA TR-FRET experiments

	Radioligand binding			TR-FRET		
Agonist	**k_{on} ($nM^{-1}\cdot min^{-1}$)[a]**	**k_{off} (min^{-1})[a]**	**RT (min)[c]**	**k_{on} ($nM^{-1}\cdot min^{-1}$)[b]**	**k_{off} (min^{-1})[b]**	**RT (min)[c]**
GnRH	0.06 ± 0.01	0.2 ± 0.02	6.3 ± 0.6	0.02 ± 0.01	0.44 ± 0.3	2.3 ± 1.6
Triptorelin	0.1 ± 0.01	0.03 ± 0.008	39 ± 12	0.1 ± 0.02	0.05 ± 0.008	21 ± 3.7
[D-Ala^6]-GnRH	0.08 ± 0.01	0.07 ± 0.01	15 ± 3.1	0.05 ± 0.007	0.07 ± 0.01	14 ± 2.3
[D-Lys^6]-GnRH	0.04 ± 0.02[#]	0.1 ± 0.04[#]	7.7 ± 2.3[#]	0.02 ± 0.01	0.25 ± 0.17	4 ± 2.6
Fertirelin	0.02 ± 0.004[#]	0.02 ± 0.001[#]	56 ± 3.1[#]	0.07 ± 0.009	0.06 ± 0.01	15 ± 2.4
Alarelin	0.09 ± 0.02	0.01 ± 0.002	77 ± 12	0.09 ± 0.009	0.03 ± 0.005	31 ± 4.8
Deslorelin	0.07 ± 0.01[#]	0.01 ± 0.002[#]	100 ± 20[#]	0.05 ± 0.005	0.02 ±0.004	44 ± 6.9
Leuprorelin	0.2 ± 0.04	0.03± 0.005	36 ± 6.4	0.03 ± 0.004	0.04 ± 0.006	26 ± 4.4
Nafarelin	0.8 ± 0.2	0.02 ± 0.003	50 ± 7.5	0.1 ± 0.02	0.03 ± 0.006	39 ± 9.8
Buserelin	0.2 ± 0.06	0.009 ± 0.003	111 ± 37	0.05 ± 0.004	0.02 ± 0.003	61 ± 10
Goserelin	0.2 ± 0.002	0.2 ± 0.03	5.6 ± 0.8	0.03 ± 0.005	0.08 ± 0.01	13 ± 2.4
Histerelin	0.3 ± 0.04	0.01 ± 0.002	83 ± 14	0.02 ± 0.002	0.02 ± 0.004	50 ± 8.8

Values are means ± SEM of at least three separate experiments performed in duplicate
[#]Values are means ± SEM of two separate experiments performed in duplicate
[a]k_{on} and k_{off} of unlabelled GnRH agonists were determined at onefold K_i concentrations
[b]k_{on} and k_{off} of unlabelled GnRH agonists were determined at 0.5, 5, 50 and 500 nM
[c]$RT = 1/k_{off}$

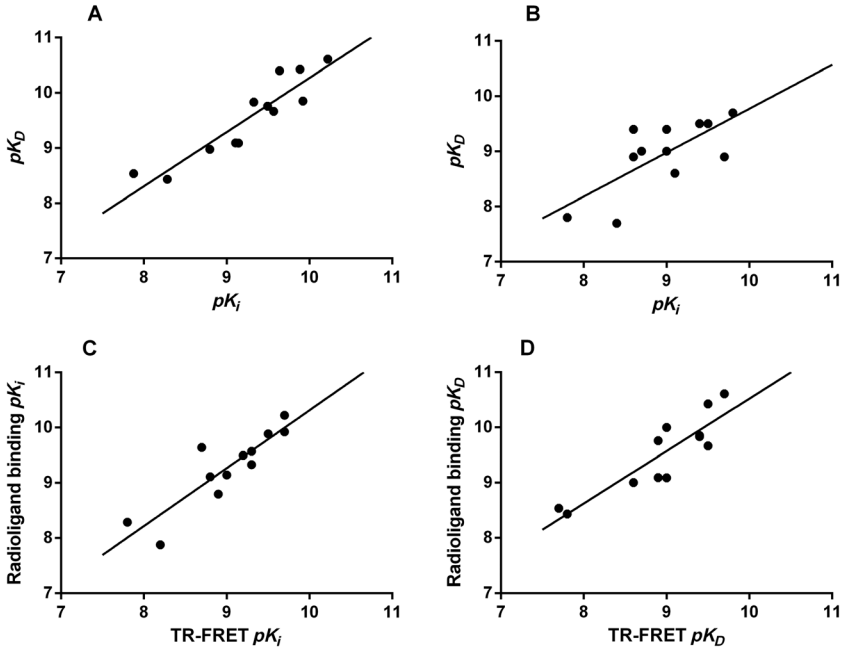

Figure 4

Correlation between affinities (pK_i) and dissociation constants (pK_D) derived from (A) radioligand binding ($r^2 = 0.9$, $P < 0.0001$) and (B) TR-FRET experiments ($r^2 = 0.5$, $P < 0.05$). (C) Correlation between affinities (pK_i) derived from radioligand binding and homogeneous time-resolved fluorescent experiments ($r^2 = 0.5$, $P < 0.05$). (D) Correlation between dissociation constants (pK_D) derived from radioligand binding and TR-FRET experiments ($r^2 = 0.8$, $P < 0.001$). In all cases, pK_i values were obtained from equilibrium displacement studies, and pK_D values were determined with competition association experiments.

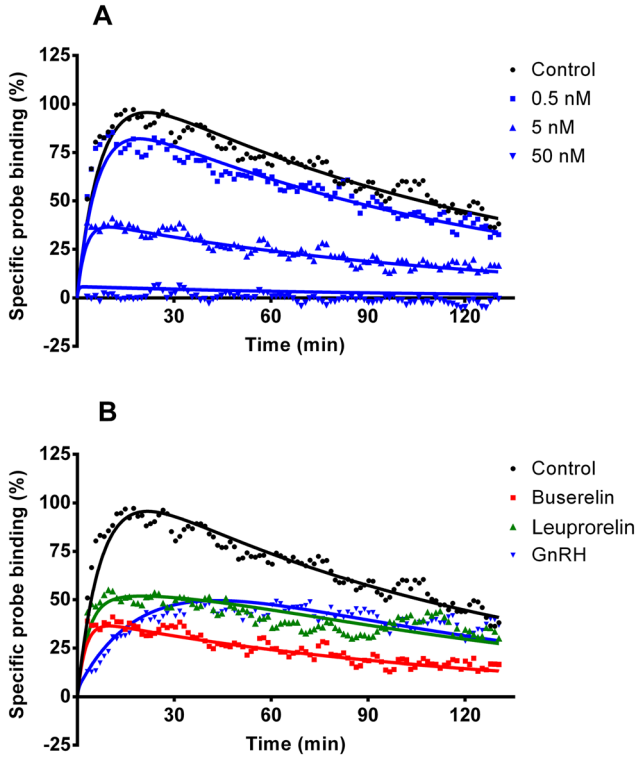

Figure 5

Competition association experiment with fluorescent probe in the absence or presence of increasing concentrations of buserelin (A) or one-concentration of unlabelled agonist that showed around 50% displacement (B). Representative graphs from one experiment performed in quadruplicate.

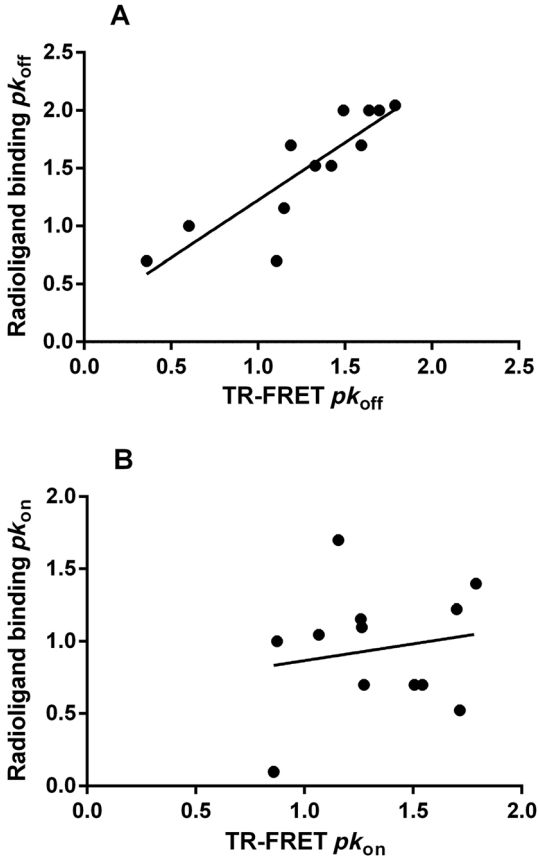

Figure 6

Correlation between the kinetic parameters obtained from radioligand-binding assays and kPCA TR-FRET experiments. (A) Dissociation rate (k_{off}) (r^2 = 0.7, $P < 0.0005$); (B) association rate (k_{on}) (r^2 = 0.03, P = 0.6).

the differences in antagonistic and kinetic properties of TAK-013 for hGnRH receptors, mouse GnRH receptors and mutated mouse GnRH receptors and found a good correlation between the degree of insurmountability in *in vitro* functional assays and the dissociation rate from the receptor. Therefore, they proposed slow receptor dissociation kinetics to be accountable for the mechanism of insurmountability of TAK-013. Similar findings were published (Sullivan *et al.*, 2006) for another series of small molecule antagonists, that is, uracils. Slowly dissociating ligands displayed insurmountable antagonism, whereas faster dissociating ligands proved to be surmountable antagonists. To determine the dissociation rates of these uracil series of antagonists, the competition association method (Motulsky and Mahan, 1984) was used with a proprietary small molecule radioligand as a tracer. Such a competition association assay has recently been applied to determine the receptor kinetics of ligands for several different GPCRs such as the adenosine A_{2A} receptor (Guo *et al.*, 2012), the muscarinic M_3 receptor (Sykes *et al.*, 2009), the chemokine receptor CCR2 (Zweemer *et al.*, 2013) and the histamine H_1 and H_3 receptor (Slack *et al.*, 2011). We were able, for the first time, to determine the kinetic parameters of 12 GnRH peptide agonists, including many marketed drugs.

Two different techniques were applied, namely, radioligand-binding studies and kPCA with a TR-FRET readout. For the former, a comparison of the radioligand's kinetic parameters obtained from traditional radioligand-binding experiments showed a good consistency with the kinetic parameters for triptorelin derived from the competition association assay (Table 2). Moreover, the kinetics of the 11 remaining GnRH agonists presented a good correlation between the kinetically derived K_D and the affinity obtained from equilibrium radioligand-binding studies (Figure 4). Secondly, we also conducted these experiments with a fluorescently labelled buserelin probe in a TR-FRET assay. This technology has already been used for examining equilibrium GPCR ligand binding (Degorce *et al.*, 2009; Zhang and Xie, 2012), and more recently, it was used to characterize the binding kinetics of the histamine H_1 receptor (Schiele *et al.*, 2014).

Comparing affinities and kinetic K_D values from both the radioligand-binding and TR-FRET assays yielded significant correlations demonstrating a good reproducibility between both techniques. The two distinct assays also proved to be very amenable to the determination of the kinetic receptor-binding parameters of (peptide) GnRH agonists. Dissociation rates, and thus residence times, between assays were in good accordance with P-values of <0.0005, while the association rates were in less agreement between techniques. It should be noted that the experimental differences between both

assays are considerable, which may have consequences for the kinetic parameters derived in the two assays. For example, the radioligand-binding studies were manually dispensed while the TR-FRET assays were performed using automated dispensing devices. It has been reported that compound handling can be an important source of assay variability (Gubler *et al.*, 2013). In addition, the kinetic binding parameters were determined using a one-concentration method for the radioligand-binding experiments, whereas the kPCA studies used five different concentrations. Another notable difference is that in the radioligand-binding studies, CHOhGnRH membranes were used, whereas the TR-FRET assays were performed with Tag-lite HEK293 GnRH cells. Packeu *et al.* (2008) discussed the differences in membrane interactions of membrane preparations and whole cells and their effects on binding kinetics for the D_{2L}-dopamine receptors. Moreover, the authors found slower dissociation rates from intact cells in comparison with membrane preparations, and they proposed that an intact cellular environment could play a role in stabilizing the D_{2L}-dopamine receptors in a particular conformation. A similar reasoning might be applicable to the GnRH receptors, although in our case, the receptor appears in a way that slows down the association rates of the peptides (Table 5). It may also be that the peptides simply have more difficulty in reaching the receptor on intact cells than on membrane fragments.

It might be argued that the assay temperature of 25°C is not representative for binding kinetics observed *in vivo*. For example, Sakai (1991) examined the effect of temperature on the dissociation of [^{125}I]-prolactin from the rabbit mammary gland prolactin receptor. They found a linear relationship between the dissociation rate and temperature with an increased dissociation rate at higher temperatures. Another study (Treherne and Young, 1988) also showed that the dissociation of [^{3}H]-QMDP from the histamine H_1 receptor was temperature-dependent, which was also true for the association rate but to a lesser extent. Arrhenius plots for both the association rate and dissociation rate of [^{3}H]-QMDP were linear between 6 and 37°C. It should be noted that, although these studies show a linear increase in dissociation rates with higher temperatures, the slope of this increase could be very different between targets and their ligands. Taken together, this indicates that the kinetic ranking of ligands for the same receptor can be expected to stay the same over different temperatures. Therefore, even though all our experiments were performed at 25°C, the results are still of great value for translation to *in vivo* outcomes.

Numerous peptide GnRH derivatives have been synthesized and studied for their so-called structure–affinity relationships, with the aim to improve their affinity, potency and/or metabolic stability (Fujino *et al.*, 1972; Monahan *et al.*, 1973; Karten and Rivier, 1986; Sealfon *et al.*, 1997; Hovelmann *et al.*, 2002; Millar *et al.*, 2004) In summary, it was established that the NH_2-terminal domain (pGlu–His–Trp–Ser) of GnRH is important for receptor binding and activation with Trp^{3} as a critical residue. In addition, the COOH-terminal domain (Pro–Gly–NH_2) is crucial for receptor binding where substitution of Pro^{9} or removal of NH_2 results in very low affinity unless the COOH-terminal tail is substituted for an ethylamide, which also improves metabolic stability. In contrast, the central domain of the peptide is less conserved, and studies show that exchange of Tyr^{5}, Leu^{7} or Arg^{8} is mostly well tolerated. The most beneficial substitution is that of Gly^{6} with a D-amino acid, which provides a more favourable conformation and in turn results in increased potency. D-amino acids at the sixth position of the peptide are therefore incorporated in all the GnRH analogues marketed. The amino acid sequences of the 12 GnRH peptides tested in this study are identical with the exception of the sixth amino acid and the carboxylic tail (Table 1). A tentative structure–kinetic relationship could be established for the carboxylic tail (i.e. substitution of the glycine amide for an ethylamide). For instance, a comparison of triptorelin and deslorelin showed 2/3-fold changes in affinity (Table 4), which was also observed in residence time. This ethylamide-induced improvement in residence time was also true to a bigger extent for goserelin and buserelin, where the affinity was improved 2-fold or 16-fold (TR-FRET and radioligand binding, respectively), while the residence time was more significantly affected, witnessed by a fivefold increase in the kPCA TR-FRET experiments and a 20-fold increase in the radioligand-binding studies. This shows that shortening the carboxylic tail of the peptide slightly increases the affinity but results in a more significant improvement in residence time. Interestingly, three decades ago, it was already speculated that buserelin has a longer residence time. In these studies, the authors proposed that the high potency and long duration of action of buserelin *in vivo* was a result of prolonged GnRH receptors binding (Yeo *et al.*, 1981; Koiter *et al.*, 1984; Koiter *et al.*, 1986). Along similar lines, Flanagan and coworkers (1998) discussed slower dissociation rates of GnRH agonists with a more hydrophobic amino acid at position 6. However, no mechanism or kinetic binding data were reported at that time.

Previously published mutagenesis studies further strengthen our hypothesis indicating the importance of the ethylamide at the carboxylic tail. Davidson and coworkers (1995) showed that the Asn$^{2.65(102)}$ residue located near the extracellular end of TM2 plays a role in ligand binding, specifically with the carboxylic tail of GnRH analogues. Mutations to alanine at this position significantly decreased the potency of GnRH analogues with Gly^{10}–NH_2 but had a lesser effect on GnRH analogues with an ethylamide tail (Davidson *et al.*, 1996; Hoffmann *et al.*, 2000; Millar *et al.*, 2004). It may be hypothesized that substitution of Gly^{10}–NH_2 with an ethylamide moiety creates less steric hindrance and increases hydrophobicity, thereby improving the fit of the agonist and thus elongating its residence time on the receptor.

In conclusion, two novel competition association assays were successfully developed and applied to determine the kinetic binding characteristics of 12 peptide agonists, including many marketed drugs targeting the GnRH receptor. All agonists proved to have high affinity for the GnRH receptor, whereas significant differences were observed in their binding kinetics. These findings provide new insights and tools for the development of improved drugs targeting the GnRH receptor by incorporating optimized kinetic binding parameters. They also suggest that bringing this knowledge on kinetics to the clinic may help in improving or adjusting treatment protocols with better patient outcomes.

Acknowledgements

This study was partly undertaken within the framework of the 'Kinetics for Drug Discovery (K4DD)' consortium. The K4DD project is supported by the Innovative Medicines Initiative Joint Undertaking (IMI JU) under grant agreement no. 115366, resources of which are composed of financial contribution from the European Union's Seventh Framework Programme (FP7/2007-2013) and EFPIA companies in kind contribution. The authors would like to acknowledge Delphine Jaga (Cisbio Bioassays) for excellent technical support.

Author contributions

I. N., F. S., V. G., K. N-R., A. E. F-M., A. P. I. and L. H. H. participated in research design. I. N., F. S. and V. G. conducted experiments. I. N., F. S. and V. G. performed data analysis. I. N., L. H. H., A.P. I., F. S., V. G. and A. E. F-M. wrote or contributed to the writing of the manuscript.

Conflict of interest

None.

References

Aguilar-Rojas A, Huerta-Reyes M, Maya-Nunez G, Arechavaleta-Velasco F, Conn PM, Ulloa-Aguirre A *et al.* (2012). Gonadotropin-releasing hormone receptor activates GTPase RhoA and inhibits cell invasion in the breast cancer cell line MDA-MB-231. BMC Cancer 12: 550–561.

Alexander SPH, Benson HE, Faccenda E, Pawson AJ, Sharman JL, Spedding M *et al.* (2013). The Concise Guide to Pharmacology 2013/14: G protein-coupled receptors. Br J Pharmacol 170: 1459–1581.

Angelucci C, Lama G, Iacopino F, Ferracuti S, Bono AV, Millar RP *et al.* (2009). GnRH receptor expression in human prostate cancer cells is affected by hormones and growth factors. Endocrine 36: 87–97.

Anthes JC, Gilchrest H, Richard C, Eckel S, Hesk D, West RE Jr *et al.* (2002). Biochemical characterization of desloratadine, a potent antagonist of the human histamine H(1) receptor. Eur J Pharmacol 449: 229–237.

Aydiner A, Kilic L, Yildiz I, Keskin S, Sen F, Kucucuk S *et al.* (2013). Two different formulations with equivalent effect? Comparison of serum estradiol suppression with monthly goserelin and trimonthly leuprolide in breast cancer patients. Med Oncol 30: 354–362.

Belchetz PE, Plant TM, Nakai Y, Keogh EJ, Knobil E (1978). Hypophysial responses to continuous and intermittent delivery of hypopthalamic gonadotropin-releasing hormone. Science 202: 631–633.

Cheng Y, Prusoff WH (1973). Relationship between inhibition constant (K1) and concentration of inhibitor which causes 50 per cent inhibition (I50) of an enzymatic-reaction. Biochem Pharmacol 22: 3099–3108.

Copeland RA, Pompliano DL, Meek TD (2006). Drug-target residence time and its implications for lead optimization. Nat Rev Drug Discov 5: 730–739.

Davidson JS, Flanagan CA, Zhou W, Becker II, Elario R, Emeran W *et al.* (1995). Identification of N-glycosylation sites in the gonadotropin-releasing hormone receptor: role in receptor expression but not ligand binding. Mol Cell Endocrinol 107: 241–245.

Davidson JS, McArdle CA, Davies P, Elario R, Flanagan CA, Millar RP (1996). Asn102 of the gonadotropin-releasing hormone receptor is a critical determinant of potency for agonists containing C-terminal glycinamide. J Biol Chem 271: 15510–15514.

Degorce F, Card A, Soh S, Trinquet E, Knapik GP, Xie B (2009). HTRF: a technology tailored for drug discovery – a review of theoretical aspects and recent applications. Curr Chem Genomics 3: 22–32.

Depalo R, Jayakrishan K, Garruti G, Totaro I, Panzarino M, Giorgino F *et al.* (2012). GnRH agonist versus GnRH antagonist in *in vitro* fertilization and embryo transfer (IVF/ET). Reprod Biol Endocrinol 10: 26.

Dowling MR, Charlton SJ (2006). Quantifying the association and dissociation rates of unlabelled antagonists at the muscarinic M3 receptor. Br J Pharmacol 148: 927–937.

Flanagan CA, Fromme BJ, Davidson JS, Millar RP (1998). A high affinity gonadotropin-releasing hormone (GnRH) tracer, radioiodinated at position 6, facilitates analysis of mutant GnRH receptors. Endocrinology 139: 4115–4119.

Fujino M, Fukuda T, Shinagaw S, White WF, Yamazaki I, Kobayasi S *et al.* (1972). Syntheses and biological-activities of analogs of luteinizing-hormone releasing hormone (Lh-Rh). Biochem Biophys Res Commun 49: 698–705.

Goericke-Pesch S, Georgiev P, Atanasov A, Albouy M, Navarro C, Wehrend A (2013). Treatment of queens in estrus and after estrus with a GnRH-agonist implant containing 4.7 mg deslorelin; hormonal response, duration of efficacy, and reversibility. Theriogenology 79: 640–646.

Gubler H, Schopfer U, Jacoby E (2013). Theoretical and experimental relationships between percent inhibition and IC50 data observed in high-throughput screening. J Biomol Screen 18: 1–13.

Guo D, Hillger JM, IJzerman AP, Heitman LH (2014). Drug-target residence time – a case for G protein-coupled receptors. Med Res Rev 34: 856–892.

Guo D, Mulder-Krieger T, IJzerman AP, Heitman LH (2012). Functional efficacy of adenosine A_{2A} receptor agonists is positively correlated to their receptor residence time. Br J Pharmacol 166: 1846–1859.

Heise CE, Sullivan SK, Crowe PD (2007). Scintillation proximity assay as a high-throughput method to identify slowly dissociating nonpeptide ligand binding to the GnRH receptor. J Biomol Screen 12: 235–239.

Heitman LH, IJzerman AP (2008). G protein-coupled receptors of the hypothalamic-pituitary-gonadal axis: a case for Gnrh, LH, FSH, and GPR54 receptor ligands. Med Res Rev 28: 975–1011.

Heitman LH, Ye K, Oosterom J, Ijzerman AP (2008). Amiloride derivatives and a nonpeptidic antagonist bind at two distinct allosteric sites in the human gonadotropin-releasing hormone receptor. Mol Pharmacol 73: 1808–1815.

Hoffmann SH, ter Laak T, Kuhne R, Reilander H, Beckers T (2000). Residues within transmembrane helices 2 and 5 of the human gonadotropin-releasing hormone receptor contribute to agonist and antagonist binding. Mol Endocrinol 14: 1099–1115.

Hovelmann S, Hoffmann SH, Kuhne R, ter Laak T, Reilander H, Beckers T (2002). Impact of aromatic residues within transmembrane helix 6 of the human gonadotropin-releasing hormone receptor upon agonist and antagonist binding. Biochemistry 41: 1129–1136.

Kakar SS, Grizzle WE, Neill JD (1994). The nucleotide-sequences of human GnRH receptors in breast and ovarian-tumors are identical with that found in pituitary. Mol Cell Endocrinol 106: 145–149.

Karten MJ, Rivier JE (1986). Gonadotropin-releasing-hormone analog design – structure-function studies toward the development of agonists and antagonists – rationale and perspective. Endocr Rev 7: 44–66.

Kohout TA, Xie Q, Reijmers S, Finn KJ, Guo Z, Zhu YF *et al.* (2007). Trapping of a nonpeptide ligand by the extracellular domains of the gonadotropin-releasing hormone receptor results in insurmountable antagonism. Mol Pharmacol 72: 238–247.

Koiter TR, Denef C, Andries M, Moes H, Schuiling GA (1986). The prolonged action of the LHRH agonist buserelin (HOE 766) may be due to prolonged binding to the LHRH receptor. Life Sci 39: 443–452.

Koiter TR, van der Schaaf-Verdonk GC, Kuiper H, Pols-Valkhof N, Schuiling GA (1984). A comparison of the LH-releasing activities of LH-RH and its agonistic analogue buserelin in the ovariectomized rat. Life Sci 34: 1597–1604.

Labrie F (2014). GnRH agonists and the rapidly increasing use of combined androgen blockade in prostate cancer. Endocr Relat Cancer 4: 301–317.

Lahlou N, Roger M, Chaussain JL, Feinstein MC, Sultan C, Toublanc JE *et al.* (1987). Gonadotropin and alpha-subunit secretion during long term pituitary suppression by D-Trp6-luteinizing hormone-releasing hormone microcapsules as treatment of precocious puberty. J Clin Endocrinol Metab 65: 946–953.

Leone Roberti Maggiore U, Scala C, Remorgida V, Venturini PL, Del Deo F, Torella M *et al.* (2014). Triptorelin for the treatment of endometriosis. Expert Opin Pharmacother 15: 1153–1179.

Lewis KA, Goldyn AK, West KW, Eugster EA (2013). A single histrelin implant is effective for 2 years for treatment of central precocious puberty. J Pediatr 163: 1214–1216.

Maillard MP, Perregaux C, Centeno C, Stangier J, Wienen W, Brunner HR *et al.* (2002). *In vitro* and *in vivo* characterization of the activity of telmisartan: an insurmountable angiotensin II receptor antagonist. J Pharmacol Exp Ther 302: 1089–1095.

Millar RP, Lu ZL, Pawson AJ, Flanagan CA, Morgan K, Maudsley SR (2004). Gonadotropin-releasing hormone receptors. Endocr Rev 25: 235–275.

Millar RP, Newton CL (2013). Current and future applications of GnRH, kisspeptin and neurokinin B analogues. Nat Rev Endocrinol 9: 451–466.

Monahan MW, Amoss MS, Anderson HA, Vale W (1973). Synthetic analogs of hypothalamic luteinizing-hormone releasing factor with increased agonist or antagonist properties. Biochemistry 12: 4616–4620.

Motulsky HJ, Mahan LC (1984). The kinetics of competitive radioligand binding predicted by the law of mass action. Mol Pharmacol 25: 1–9.

Packeu A, De Backer JP, Van Liefde I, Vanderheyden PM, Vauquelin G (2008). Antagonist-radioligand binding to D2L-receptors in intact cells. Biochem Pharmacol 75: 2192–2203.

Pawson AJ, Sharman JL, Benson HE, Faccenda E, Alexander SP, Buneman OP *et al.* (2014). The IUPHAR/BPS Guide to PHARMACOLOGY: an expert-driven knowledgebase of drug targets and their ligands. Nucl Acids Res 42 (Database Issue): D1098–D1106.

Romero E, Velez de Mendizabal N, Cendros JM, Peraire C, Bascompta E, Obach R *et al.* (2012). Pharmacokinetic/pharmacodynamic model of the testosterone effects of triptorelin administered in sustained release formulations in patients with prostate cancer. J Pharmacol Exp Ther 342: 788–798.

Sakai S (1991). Effect of hormones on dissociation of prolactin from the rabbit mammary gland prolactin receptor. Biochem J 279 (Pt 2): 461–465.

Schiele F, Ayaz P, Fernandez-Montalvan A (2014). A universal, homogenous assay for high throughput determination of binding kinetics. Anal Biochem 486C: 42–49.

Sealfon SC, Weinstein H, Millar RP (1997). Molecular mechanisms of ligand interaction with the gonadotropin-releasing hormone receptor. Endocr Rev 18: 180–205.

Slack RJ, Russell LJ, Hall DA, Luttmann MA, Ford AJ, Saunders KA *et al.* (2011). Pharmacological characterization of GSK1004723, a novel, long-acting antagonist at histamine H(1) and H(3) receptors. Br J Pharmacol 164: 1627–1641.

Smith DA, Jones BC, Walker DK (1996). Design of drugs involving the concepts and theories of drug metabolism and pharmacokinetics. Med Res Rev 16: 243–266.

Smith PK, Krohn RI, Hermanson GT, Mallia AK, Gartner FH, Provenzano MD *et al.* (1985). Measurement of protein using bicinchoninic acid. Anal Biochem 150: 76–85.

Stojilkovic SS, Reinhart J, Catt KJ (1994). Gonadotropin-releasing hormone receptors: structure and signal transduction pathways. Endocr Rev 15: 462–499.

Sullivan SK, Hoare SR, Fleck BA, Zhu YF, Heise CE, Struthers RS *et al.* (2006). Kinetics of nonpeptide antagonist binding to the human gonadotropin-releasing hormone receptor: implications for structure-activity relationships and insurmountable antagonism. Biochem Pharmacol 72: 838–849.

Swinney DC (2004). Biochemical mechanisms of drug action: what does it take for success? Nat Rev Drug Discov 3: 801–808.

Swinney DC (2009). The role of binding kinetics in therapeutically useful drug action. Curr Opin Drug Discov Devel 12: 31–39.

Sykes DA, Dowling MR, Charlton SJ (2009). Exploring the mechanism of agonist efficacy: a relationship between efficacy and agonist dissociation rate at the muscarinic M3 receptor. Mol Pharmacol 76: 543–551.

Tashkin DP (2005). Is a long-acting inhaled bronchodilator the first agent to use in stable chronic obstructive pulmonary disease? Curr Opin Pulm Med 11: 121–128.

Treherne JM, Young JM (1988). Temperature-dependence of the kinetics of the binding of [3H]-(+)-N-methyl-4-methyldiphenhydramine to the histamine H1-receptor: comparison with the kinetics of [3H]-mepyramine. Br J Pharmacol 94: 811–822.

Tummino PJ, Copeland RA (2008). Residence time of receptor-ligand complexes and its effect on biological function. Biochemistry 47: 5481–5492.

Vauquelin G, Van Liefde I (2006). Slow antagonist dissociation and long-lasting *in vivo* receptor protection. Trends Pharmacol Sci 27: 356–359.

von Alten J, Fister S, Schulz H, Viereck V, Frosch KH, Emons G *et al.* (2006). GnRH analogs reduce invasiveness of human breast cancer cells. Breast Cancer Res Tr 100: 13–21.

Yeo T, Grossman A, Belchetz P, Besser GM (1981). Response of luteinizing hormone from columns of dispersed rat pituitary cells to a highly potent analogue of luteinizing hormone releasing hormone. J Endocrinol 91: 33–41.

Zhang R, Monsma F (2009). The importance of drug-target residence time. Curr Opin Drug Discov Devel 12: 488–496.

Zhang R, Xie X (2012). Tools for GPCR drug discovery. Acta Pharmacol Sin 33: 372–384.

Zweemer AJ, Nederpelt I, Vrieling H, Hafith S, Doornbos ML, de Vries H *et al.* (2013). Multiple binding sites for small-molecule antagonists at the CC chemokine receptor 2. Mol Pharmacol 84: 551–561.

Supporting Information

Additional Supporting Information may be found in the online version of this article at the publisher's web-site:

http://dx.doi.org/10.1111/bph.13322

Figure Saturation equilibrium binding of fluorescent 1
Saturation equilibrium binding of fluorescent buserelin probe to Tag-lite™ GnRH cells (IC_{50} = 5.9 nM, r^2 = 0.99). Representative graph from one experiment performed in duplicate.

Figure Saturation equilibrium binding of fluorescent 2
Association and dissociation kinetics of five concentrations of fluorescent buserelin probe to Tag-lite™ GnRH cells. Representative graph from one experiment performed in duplicate.

Figure Saturation equilibrium binding of fluorescent 3
kPCA traces of the GnRH peptide agonists analysed. Four concentrations (0.5, 5, 50 and 500 nM) were examined. Representative graphs from one experiment performed in duplicate.